



Nanomaterial Fungicides: In Vitro and In Vivo Antimycotic Activity of Cobalt and Nickel Nanoferrites on Phytopathogenic Fungi

Sharma, P., Sharma, A., Sharma, M., Bhalla, N., Estrela, P., Jain, A., Thakur, P., & Thakur, A. (2017). Nanomaterial Fungicides: In Vitro and In Vivo Antimycotic Activity of Cobalt and Nickel Nanoferrites on Phytopathogenic Fungi. *Global Challenges*, 1(9), 1700041. <https://doi.org/10.1002/gch2.v1.9>

[Link to publication record in Ulster University Research Portal](#)

Published in:
Global Challenges

Publication Status:
Published (in print/issue): 15/12/2017

DOI:
[10.1002/gch2.v1.9](https://doi.org/10.1002/gch2.v1.9)

Document Version
Author Accepted version

General rights

Copyright for the publications made accessible via Ulster University's Research Portal is retained by the author(s) and / or other copyright owners and it is a condition of accessing these publications that users recognise and abide by the legal requirements associated with these rights.

Take down policy

The Research Portal is Ulster University's institutional repository that provides access to Ulster's research outputs. Every effort has been made to ensure that content in the Research Portal does not infringe any person's rights, or applicable UK laws. If you discover content in the Research Portal that you believe breaches copyright or violates any law, please contact pure-support@ulster.ac.uk.

Article type: Full Paper

Title: Nanomaterial Fungicides: *In vitro* and *in vivo* antimycotic activity of cobalt and nickel nanoferrites on phytopathogenic fungi

Parul Sharma^a, Adikshita Sharma^b, Monica Sharma^b, Nikhil Bhalla^{c,d}, Pedro Estrela^c, Aditya Jain^e, Preeti Thakur^f, Atul Thakur^{g*}*

^aNanotechnology Wing, Innovative Science Research Society, Shimla 171002 India

^bDepartment of Plant Pathology, Dr. Y.S. Parmar University of Horticulture and Forestry, Nauni, Solan H.P., India, 173230

^cDepartment of Electronic and Electrical Engineering, University of Bath, Bath BA2 7AY, United Kingdom

^dMicro/Bio/Nanofluidics Unit, Okinawa Institute of Science and Technology Graduate University (OIST) 1919-1 Tancha, Onna, Kunigami District, Okinawa Prefecture 904-0412 Japan

^eInstitute of Energy Efficiency, University of California Santa Barbara, Santa Barbara, CA 93106-9560, USA

^fAmity School of Applied Sciences, Amity University Gurgaon, Haryana, India, 122413

^gAmity Center of Nanotechnology, Amity University Gurgaon, Haryana, India, 122413

Emails of corresponding authors: N.B. nikhil.bhalla@bath.edu; nikhil.bhalla@oist.jp ; A.T. atulphysics@gmail.com

Abstract

Recent advances in engineering led to the fabrication of nanomaterials with unique properties targeted toward specific applications. The use of nanotechnology in agriculture, in particular for plant protection and production, is an under-explored area in the research community. Fungal diseases are one of the leading causes of crop destruction and, in this context, the antifungal effect of nanoparticles of cobalt and nickel ferrite against phytopathogenic fungi are reported here. As a proof of concept, it was also shown how such nanoparticles can be used as fungicides in plants. The developed cobalt and nickel ferrite nanoparticles (CoFe_2O_4 and NiFe_2O_4) were successfully tested for antimycotic activity against three plant-pathogenic fungi: *Fusarium oxysporum*, *Colletotrichum gloeosporioides* and *Dematophora necatrix*. In addition, it is also observed that these ferrite nanoparticles reduce the incidence of *Fusarium* wilt in capsicum. The study suggests that nanoparticles of CoFe_2O_4 and NiFe_2O_4 could be used as an effective fungicide in plant disease management.

1. Introduction

Plant diseases have caused severe losses to humans ever since the beginning of agriculture¹. Organisms that cause infectious diseases in plants mainly include fungi, bacteria, viruses, protozoa and plant parasites². Among these organisms, fungi are responsible for the most damaging diseases in plants³. It is estimated that around 85% of all plant diseases are fungal in nature. To combat fungi, farmers have been evolving their practices by using various types of chemical fungicides such as mancozeb⁴, kitazin⁵, copper hydroxide⁶ and many others⁷. However, fungi respond to the use of fungicides by developing resistance against the compounds⁸. The evolution of fungicide resistance can either be sudden or gradual. Consequently, farmers either use a combination of more than one fungicide or use excessive fungicides to control the disease. This can lead to either damaged crops or to residues of

fungicides remaining in the plant, some of which are harmful to human health⁹⁻¹¹. Therefore, with the growing demand to control pathogens, especially fungi, there is an urgent need to tackle the excessive usage of fungicides by finding less harmful alternatives.

Nanoparticle (NP) materials have received increasing attention due to their unique physical and chemical properties, which differ significantly from their conventional macroscale counterparts¹². The antimicrobial effect of various NP materials such as silver¹³, copper¹⁴, titanium dioxide¹⁵, zinc oxide¹⁶ and magnesium oxide¹⁷ has been demonstrated. However, most of these materials so far found limited practical use in agriculture mainly due the cytotoxic effects that they produce in plants. While NPs kill pathogens or the diseased plant cells, they also include a risk of damaging normal cells of plants. For practical applications, the use of nanoparticles as pesticides will be preferable only if the nanoparticles are selective in killing pathogens without damaging the plant.

This work successfully demonstrates the antimycotic effect of nanoparticles of pure cobalt and nickel ferrite on the growth of three important plant pathogenic fungi: *Fusarium oxysporum* (Schlectend) Emend. Synder and Hansen, *Colletotrichum gloeosporioides* (Penz.) Penz. & Sacc. and *Dematophora necatrix* Hartig. *Fusarium oxysporum* and *Colletotrichum gloeosporioides* are among the top ten fungal pathogens for molecular plant pathology¹⁸. *Fusarium oxysporum* is a ubiquitous soil borne pathogen which causes vascular wilt on a wide range of plants¹⁹. The *Fusarium oxysporum* species complex comprises different formae speciales (f. sp.), which collectively infect more than 100 different hosts, provoking severe losses in crops. *Colletotrichum gloeosporioides* is one of the most common and important plant pathogenic fungi. Virtually every crop grown throughout the world is susceptible to one or more species of *Colletotrichum*²⁰. This fungus causes anthracnose spots and blights of aerial plant parts and post-harvest rots. Members of this genus also cause major loss to economically important crops, especially fruits, vegetables and ornamentals plants. On the other hand, *Dematophora necatrix* causes white root rot in trees bearing fruits, such as the

apple tree.²¹ We find that ferrite nanoparticles are effective in reducing the mycelia growth of these fungi. Moreover, the activity of NPs was successfully tested in plants. The ferrite nanoparticles reduce the incidence of *Fusarium* wilt in capsicum plants. The wilt in capsicum plant was reduced by killing the *Fusarium oxysporum* without affecting the normal cells of plant, henceforth curing the wilting of capsicum plant. This work reports for the first time, to the best of our knowledge, the antifungal effect of nanoparticles of cobalt and nickel ferrite against phytopathogenic fungi and experimental demonstration of their use in plants.

2. Results and Discussion

2.1. TEM

TEM images of CoFe_2O_4 and NiFe_2O_4 nanoferrites synthesized at 800°C are shown in Figure 1 (a) and (b). The formation of ferrites is seen to be spherical and uniform with an average size of 25 nm. This is in close agreement with the XRD measurements discussed in later sections. The powder appears to be non-agglomerated and the particle size is narrowly and uniformly distributed. Thus, it can be inferred that the nucleation occurs as a slow event, resulting in the uniform distribution of particles.²²

2.2. XRD

The XRD patterns of cobalt and nickel nanoferrites sintered at 800°C are shown in Figure 2 (a) and (b). The planes at (220), (311), (400), (511) and (440) confirmed the formation of spinel structured cubic cobalt ferrite JCPDS Card No. 22-1086 and nickel ferrite JCPDS Card No. 10-0325 with no other phases or impurities present^{23,24}. The average crystalline size **D** of cobalt and nickel nanoferrite sintered at 800°C (for the most prominent peak (311)) is calculated by using Scherer's formula as:²⁵⁻²⁶

$$D = \frac{0.9\lambda}{\beta \cos \theta} \quad (1)$$

Here λ is the wavelength of Cu ($K\alpha$) and β is the full width at half maxima. The average

crystallite size of cobalt and nickel nanoferrite pre-sintered at 700°C is found to be 22 nm. The broad peaks in XRD pattern indicate finite crystal size of cobalt and nickel nanoferrites.

2.3. Raman Spectroscopy

Figure 3 shows that the samples have more than five Raman active modes, as predicted by group theory in the normal spinel structure.²⁷ The bands were observed at (289, 303, 313 cm^{-1}), (443, 468, 464, 473 cm^{-1}) and (673, 679, 681, 689 cm^{-1}) which are consistent with the predicted Raman active modes ($A_{1g}+E_g+3T_{2g}$) by the group theory. 1-D, E, 2-D, T, 3-D and g stands for symmetric vibration. All Raman modes are observed at ambient temperature condition and are composed of motion of oxygen anions and both A and B site cations. A_{1g} mode is due to the symmetric stretching of oxygen anions, E_g modes occur due to symmetric bending of oxygen anions, whereas T_{2g} mode is the result of asymmetric stretching of oxygen anions with respect to A-site and B-site cations.

2.4. FTIR

According to Waldron²⁸, in ferrites with formula $M\text{Fe}_2\text{O}_4$, where M designates a divalent metal, two absorption bands occur from interatomic vibrations for the stretching of bonds between octahedral or tetrahedral metal ions and oxide ions. The band with the higher wave number observed in the range 580–591 cm^{-1} corresponds to the intrinsic stretching vibrations of the metal at the tetrahedral site whereas the other band around the range 400–475 cm^{-1} is attributed to the octahedral-metal stretching confirming the formation of inverse spinel CoFe_2O_4 and NiFe_2O_4 nanoferrites (Figure 4 (a) and (b)). The difference in the absorption position in octahedral and tetrahedral complexes of $M\text{Fe}_2\text{O}_4$ crystals is due to the different distance between $\text{Fe}^{3+}-\text{O}^{2-}$ in the octahedral and tetrahedral sites.²⁷ The strong bond between Fe^{3+} cations with O^{2-} ions at the tetrahedral site due to a difference in electronegativity, resulted in the lowest state of energy.

2.5. Effect of CoFe₂O₄ and NiFe₂O₄ nanoparticles on mycelial growth of *Colletotrichum gloeosporioides*

It was revealed from the study that different concentrations of nanoparticles of CoFe₂O₄ and NiFe₂O₄ ferrites had inhibitory effect on mycelia growth of *Colletotrichum gloeosporioides* (Table 1). The inhibition in mycelial growth varies from 39.45% to 81.39% in different concentrations of nanoparticles of cobalt and nickel ferrite. The maximum inhibition of 81.39% and 78.91% in mycelial growth was found at 500 ppm of nickel and cobalt nanoparticles, respectively. It was followed by 78.06% and 77.23% at 400 ppm, followed by 61.94% and 56.67% at 300 ppm of nickel and cobalt nanoparticles, respectively. Least inhibition in mycelia growth (39.45%) was observed at 100 ppm of cobalt ferrite nanoparticles followed by 100 ppm of nickel ferrite nanoparticles. Interestingly, there was an induction of conidia formation at 500 ppm of nanoparticles of nickel (Figure 5). Under certain conditions some fungi undergo microcycle conidiation whereby sporulation occurs directly after spore germination without, or with greatly reduced mycelia growth. Microcycle conidiation of certain fungi may be induced by high-temperature stress, nutrient depletion or other factors inhibiting vegetative development. The nanoparticles of nickel might have created stress in cultures of *C. gloeosporioides* which results in microcycle conidiation.

2.6. Effect of CoFe₂O₄ and NiFe₂O₄ nanoparticles on mycelial growth of *Dematophora necatrix*

Different concentrations of nanoparticles of cobalt and nickel ferrite caused inhibition in the mycelial growth of *Dematophora necatrix* (Table 1). The highest mycelial growth inhibition was found at a concentration of 500 ppm followed by 400 ppm, 300 ppm, 200 ppm and 100 ppm concentrations of nanoparticles of cobalt and nickel ferrite. The mycelial growth inhibition varies from 93.33% to 39.44% in different concentrations of nanoparticles of cobalt and nickel ferrites. Maximum inhibition of 93.33% in mycelia growth was found at 500 ppm

of nanoparticles of nickel ferrite followed by 88.90% with 500 ppm of nanoparticles of cobalt ferrite.

2.7. Effect of CoFe_2O_4 and NiFe_2O_4 nanoparticles on mycelial growth of *Fusarium oxysporum*

It was revealed from the study that the different concentrations of ferrite nanoparticles of CoFe_2O_4 and NiFe_2O_4 had inhibitory effects against mycelia growth of *F. oxysporum* (Table 1). Highest mycelial growth inhibition (89.45%) was found at 500 ppm of nickel ferrite nanoparticles (Fig 4c). It was followed by 87.62% and 83.33% mycelia growth inhibition at 500 ppm of cobalt nanoparticles and 400 ppm nickel ferrite nanoparticles. Least inhibition in mycelia growth was found at 100 ppm of CoFe_2O_4 ferrite nanoparticles (39.44%) followed by 100 ppm of nickel nanoparticles (43.61%). These results were in accordance with Ahmed *et al.*²⁹ in which nickel nanoparticles at the concentration of 100 ppm caused 60.23% and 59.77% inhibition in mycelia growth of *F. oxysporum* f. sp. *lactucae* and *F. oxysporum* f. sp. *lycopersici*, respectively.

2.8. Management of *Fusarium* wilt of capsicum under pot culture conditions

Nanoparticles of CoFe_2O_4 and NiFe_2O_4 were evaluated for their efficacy against *Fusarium* wilt of capsicum in sick pots and the data indicated that different concentrations of nanoparticles reduced the disease incidence of *Fusarium* wilt of capsicum (Table 2). However, no disease incidence was recorded at 500 ppm concentration of NiFe_2O_4 ferrite nanoparticles (Figure 6). Low disease incidence (9.52%) was recorded at 400 ppm of NiFe_2O_4 ferrite nanoparticles and at 500 ppm of CoFe_2O_4 ferrite nanoparticles. It was followed by 23.80% and 28.57% disease incidence at 300 ppm of NiFe_2O_4 ferrite nanoparticles and 400 ppm of CoFe_2O_4 ferrite nanoparticles respectively. These results clearly show that the seedling treatment with 500 ppm of NiFe_2O_4 ferrite nanoparticles resulted in complete disease

reduction whereas seedling treatment with 400 ppm of NiFe_2O_4 ferrite nanoparticles and 500 ppm of CoFe_2O_4 resulted in 90.49% disease reduction. CoFe_2O_4 and NiFe_2O_4 ferrite nanoparticles at 100 and 200 ppm were found ineffective against the disease and resulted in less than 50% disease reduction. The effectiveness of nickel nanoparticles by soil drench application resulted in disease reduction of *Fusarium* wilt of tomato and lettuce that disease²⁹. Nanoparticles have a vast surface to volume ratio which significantly enhances their property of cell membrane permeability³⁰. The nanoparticles can be used as new antimicrobial agents and an alternative to synthetic fungicide to delay or inhibit the growth of many pathogens species because of their multiple modes of inhibition. Nanoparticles have high reactivity (for their target sites) and hence affect the activity of microorganisms even at very low concentrations. This observation of strong inhibitory effects of ferrite nanoparticles *in vitro* on these fungi, opens new opportunities to develop novel agro-nanotech innovative products for plant disease management.

3. Conclusion

The discovery and development of novel fungicides is important to combat the newly emerging resistant strains of pathogenic fungi. The present study shows the antimycotic efficacy of nanoparticles of CoFe_2O_4 and NiFe_2O_4 against *Fusarium oxysporum*, *Colletotrichum gloeosporioides* and *Dematophora necatrix*. In addition, the present study also demonstrates that nanoparticles of CoFe_2O_4 and NiFe_2O_4 have the potential to reduce the disease incidence of *Fusarium* wilt of capsicum and could be used for its management. Results at the micro and macro level suggest that nanoparticles of CoFe_2O_4 and NiFe_2O_4 could be used as an effective fungicide in plant disease management programs.

4. Experimental Section

4.1. Synthesis of CoFe_2O_4 and NiFe_2O_4 nanoparticles

Nickel and cobalt ferrites of composition CoFe_2O_4 and NiFe_2O_4 were prepared separately by a co-precipitation method³¹. High purity nickel chloride hexahydrate, cobalt chloride-hexahydrate and iron (III) chloride hexahydrate were taken in the proper stoichiometric proportions and dissolved in a boiling solution of 0.40 M NaOH under vigorous stirring for 30 minutes. After the suspension was cooled to room temperature, the precipitate was washed carefully with distilled water several times until pH 7 was obtained and then centrifuged to get the residue. This residue was dried in an electrical oven at 50°C overnight. The powders were calcinated in a muffle furnace at 800°C for 3 h at a heating and cooling rate of 200°C/h.

4.2. TEM

The transmission electron microscopy (TEM) characterizations were carried out using a 80 kV Transmission electron microscope (Model JEOL USA 2100F). Nanoparticles were mixed with distilled water, shaken well and put on copper grids for drying, before the TEM experiments.

4.3. XRD

XRD data was obtained using a BRUKER AXS D8 Advance, equipped with a Vante-1 detector using $\text{CuK}\alpha$ radiation ($\lambda = 1.5318 \text{ \AA}$). The instrument was setup to flatplate mode with a shallow and narrow sample holder that enabled collection of data from the powdered nanoparticles.

4.4. Raman Spectroscopy

Raman spectroscopy provides the structural properties of materials and to identify the microscopic vibrations caused by the slight structure distortion. Micro Raman scattering was used to study the structural stability of cobalt sintered nanoferrites. This characterization was done on HORIBA JOBIN VYON LABRAMHR under the illumination with 488 nm line Argon ion laser at 25 mW laser power.

4.5. FTIR

In order to obtain the FTIR spectra, nanoparticles were placed on a diamond attenuated total reflectance (ATR) FTIR instrument, Perkin Elmer, USA. Potassium bromide (KBr) was added as binder in small amounts to CoFe_2O_4 and NiFe_2O_4 nanoferrites samples to form a pellet. FTIR spectra of CoFe_2O_4 and NiFe_2O_4 nanoferrite samples sintered at 800°C were recorded in the range of range $400\text{-}2000\text{ cm}^{-1}$.

4.6. *In vitro* antifungal activity of CoFe_2O_4 and NiFe_2O_4 ferrite nanoparticles

The efficacy of nanoparticles of CoFe_2O_4 and NiFe_2O_4 were evaluated against different phytopathogenic fungi, namely *Colletotrichum gloeosporioides*, *Fusarium oxysporum* and *Dematophora necatrix*. The active cultures of fungi were procured from the Department of Plant Pathology, Dr. Y.S. Parmar University of Horticulture Forestry, Solan, India and were maintained and multiplied on potato dextrose agar medium. The CoFe_2O_4 and NiFe_2O_4 nanoparticles were tested *in vitro* by using the Poisoned Food Technique³²⁻³³ in Completely Randomized Design (CRD) to study the inhibitory effect on mycelia growth of different fungi. The nanoparticles were evaluated at different concentrations i.e., 100 ppm, 200 ppm, 300 ppm, 400 ppm and 500 ppm against the tested plant pathogenic fungi. Each treatment was done in five replicates. Double strength potato dextrose agar medium was prepared in distilled water and sterilized in an autoclave at 15 psi pressure and 121°C for 20 minutes. Simultaneously, double concentrations of nanoparticles were also prepared in sterilized distilled water and

sonicated for 30 minutes to make the colloidal solution of nanoparticles. The colloidal solution of nanoparticles was mixed with double strength potato agar medium aseptically to achieve the desired concentrations and poured into Petri plates. After the solidification of medium, these plates were inoculated with the mycelial bit of 2 mm diameter of different plant-pathogenic fungi taken from actively growing 5-days old culture. A control treatment was also maintained in which only plain sterilized distilled water was added to double strength medium. The inoculated plates were incubated at $28 \pm 1^\circ \text{C}$. The observation was recorded in the form of radial growth of plant-pathogenic fungi in millimeter (mm) daily until the control plates were fully covered with the mycelium or for 7 days. The percent growth inhibition in mycelia growth was calculated using equation 1 as described by Vincent et. al.³³

$$I = \frac{C - T}{C} \times 100 \quad (2)$$

where, I is per cent mycelia growth inhibition, C is Mycelial growth of fungus in control (mm) and T is Mycelial growth of fungus in treatment (mm). The differences exhibited by the treatments in experiment were tested for their significance by employing Completely Randomized Design (CRD) as per the details given by Gomez and Gomez³⁴.

4.7. *In vivo* evaluation of antifungal activity of CoFe_2O_4 and Ni_2FeO_4 ferrite nanoparticles

To study the efficacy of CoFe_2O_4 and NiFe_2O_4 nanoparticles against *Fusarium* wilt of capsicum, an experiment was conducted in sick pots.

4.7. 1. Preparation of sick pots

Plastic pots (10 cm diameter) were filled with sterilized soil at 500 g/pot. Thereafter soil was inoculated with 10 g mass culture of *F. oxysporum* f. sp. *capsici*, which was grown in a corn:sand meal (3:1) medium. Plastic pots filled without inoculum served as control. After

inoculation, the soil was sprayed with sterilized water and kept covered with a polythene sheet for 7 days to build up inoculums level in the pots.

4.8. Evaluation of CoFe₂O₄ and Ni₂FeO₄ nanoparticles under pot culture conditions:

Seedlings (35-40 days old) of capsicum cv. ‘Solan Bharpur’ were treated by root dip treatment in solution of different concentration of CoFe₂O₄ and NiFe₂O₄ nanoparticles for 45 minutes. Treated seven seedlings were transplanted in each pot. Experiment was conducted in a Completely Randomized Design (CRD). Each treatment was replicated thrice and suitable control was also maintained. After transplanting pots were incubated in plant growth chamber at 25±2°C temperature maintaining 70-80% relative humidity till the symptoms appeared in the control treatment. Observations were recorded on a number of wilted plants and disease incidence was calculated by following formula given by:

$$\text{Disease incidence (\%)} = \frac{\text{Number of infected plants}}{\text{Total number of plants observed}} \times 100 \quad (3)$$

The data on disease reduction over control was calculated by the formula proposed by Vincent *et al.*³¹.

Received: ((will be filled in by the editorial staff))

Revised: ((will be filled in by the editorial staff))

Published online: ((will be filled in by the editorial staff))

References

- 1) J. L. Dangl, J. D. Jones, *Nature* **2001**, *411*, 826-833.
- 2) A. H. C. van Bruggen, M. R. Finckh, *Annu. Rev. Phytopathol.* **2016**, *54*, 1-30.
- 3) T. Giraud, P. Gladieux, S. Gavrillets, *Trends Ecol. Evolut.* **2010**, *25*, 387-395.
- 4) A. V. A. Pirozzi, A. Stellavato, A.L. Gatta, M. Lamberti, C. Schiraldi, *Toxicol. Lett.* **2016**, *249*, 1-4.
- 5) R. J. Bass, R.C. Koch, H.C. Richards, J.E. Thorpe, *J. Agric. Food Chem.* **1981**, *29*, 576-579.

- 6) J.L. Capinera, K. Dickens, *Crop Prot.* **2016**, 83, 76-82.
- 7) G.D. Lyon, T. Reglinski, A. C. Newton, *Plant Pathol.* **1995**, 44, 407-427.
- 8) T. Wiesner-Hanks, R. Nelson, *Annu. Rev. Phytopathol.* **2016**, 54, 229-252.
- 9) J. Lundqvist, B. Hellman, A. Oskarsson, *Food Chem. Toxicol.* **2016**, 91, 36-41.
- 10) Y. Shukla, A. Arora, *J. Environ. Pathol., Toxicol. Oncol.* **2001**, 20, 127-131.
- 11) N.N. Ragsdale, H.D. Sisler, *Annu. Rev. Phytopathol.* **1994**, 32, 545-557.
- 12) N. Phogat, S.A. Khan, S. Shankar, I. Uddin, *Adv. Mat. Lett.* **2016**, 7, 3-12.
- 13) A. Panáček, M. Kolář, R. Večeřová, R. Prucek, J. Soukupová, V. Kryštof, P. Hamal, R. Zbořil, L. Kvítek, *Biomaterials* **2009**, 30, 6333-6340.
- 14) P. Kanhed, S. Birla, S. Gaikwad, A. Gade, A. B. Seabra, O. Rubilar, N. Duran, M. Rai, *Mater. Lett.* **2014**, 115, 13-17.
- 15) F. M. Gutierrez, P. L. Olive, A. Banuelos, E. Orrantia, N. Nino, E. M. Sanchez, F. Ruiz, H. Bach, Y. Av-Gay, *Nanomed. Nanotechnol. Biol. Med.* **2010**, 6, 681-688.
- 16) L. He, Y. Liu, A. Mustapha, M. Lin, *Microbiol. Res.* **2011**, 166, 207-215.
- 17) A.H. Wani, M. A. Shah, *J. Appl. Pharm. Sci.* **2012**, 2, 40-44.
- 18) R. Dean, J.A. L. Van-kan, Z. A. Pretorius, K. E. H. Kosack, A. D. Pietro, P. D. Spanu, J. J. Rudd, M. Dickman, R. Kahmann, J. Ellis, G. D. Foste, *Mol. Plant Pathol.* **2012**, 13, 414-430.
- 19) I. Vlaardingerbroek, B. Beerens, S.M. Schmidt, B.J. Cornelissen, M. Rep, *Mol. Plant Pathol.* **2016**, 17, 1455-1466.
- 20) L. Penet, E. Barthe, A. Alleyne, and J. M. Blazy, *Crop Prot.* **2016**, 88, 7-17.
- 21) A. Szejnberg, Z. Madar, *Plant Dis.* **1980**, 64, 662-664.
- 22) S. Thakur, A. Pathania, P. Thakur, A. Thakur, *Ceram. Int.*, **2015**, 41, 5072-5078.
- 23) K. Rana, P. Thakur; P. Sharma, M. Tomar, V. Gupta, A. Thakur *Ceram. Int.* **2015**, 41, 4492-4497.
- 24) A.C.F.M. Costa, A.M.D. Leite, H.S. Ferreira, R.H.G.A. Kiminami, S. Cavac, L. Gama, *J. Euro. Ceram. Soc.* **2008**, 28, 2033-2037.
- 25) A. Thakur, P. Thakur, J-H. Hsu, *J. Alloys Compd.* **2011**, 509, 5315-5319
- 26) P. Mathur, A. Thakur, M. Singh, *Int. J. Mod. Phys. B* **2009**, 23, 2523-2533.
- 27) P. Sharma, P. Thakur, J-L Mattei, P. Queffelec, A. Thakur, *J. Magn. Magn. Mater.* **2016**, 407, 17-23
- 28) R. D. Waldron, *Phys. Rev.* **1955**, 99, 1727-1735.
- 29) I.S.A. Ahmed, D.R. Yadav, Y.S. Lee, *Int. J. Innov. Res. Sci. Eng. Technol.* **2016**, 5, 7378-7385.
- 30) M.S. Nejad, G.H.S. Bonjar, M. Khatami, A. Amini, S. Aghighi, *IET Nanobiotechnology.* **2016**, 11, 236-240.
- 31) A. Pathania, K. Rana, N. Bhalla, P. Thakur, P. Estrela, J.L. Mattei, P. Queffelec, A. Thakur *J. Mater. Sci. Mater. Electron.* **2017**, 28, 679-685.
- 32) J.B. Sinclair, O.D. Dhingra, *Basic plant pathology methods*, CRC press, Boca Raton, USA, **1995**, p. 267.
- 33) J. M. Vincent, *Nature* **1947**, 159, 850.
- 34) K.A. Gomez, A.A. Gomez, *Statistical Procedures for Agricultural Research*, John Wiley & Sons, New York, USA, **1984**, p.8

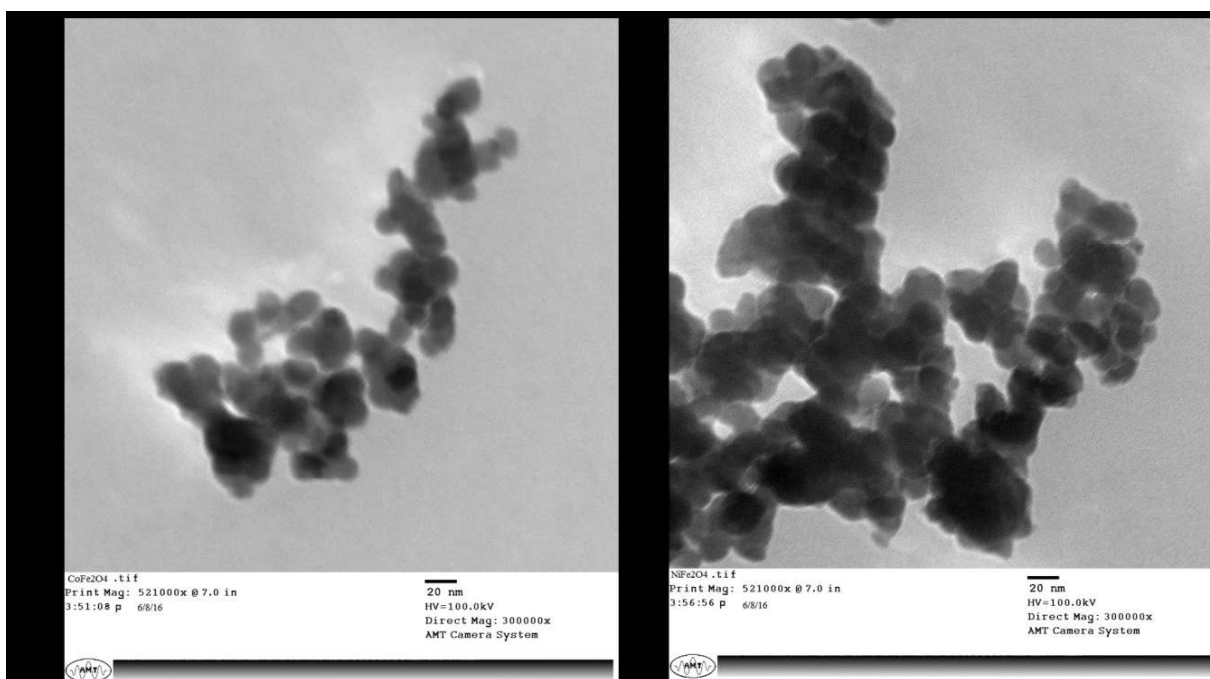


Figure 1. TEM images of (a) CoFe_2O_4 and (b) NiFe_2O_4 . Both nanoferrites show spherical nanostructures with an average size of 25nm.

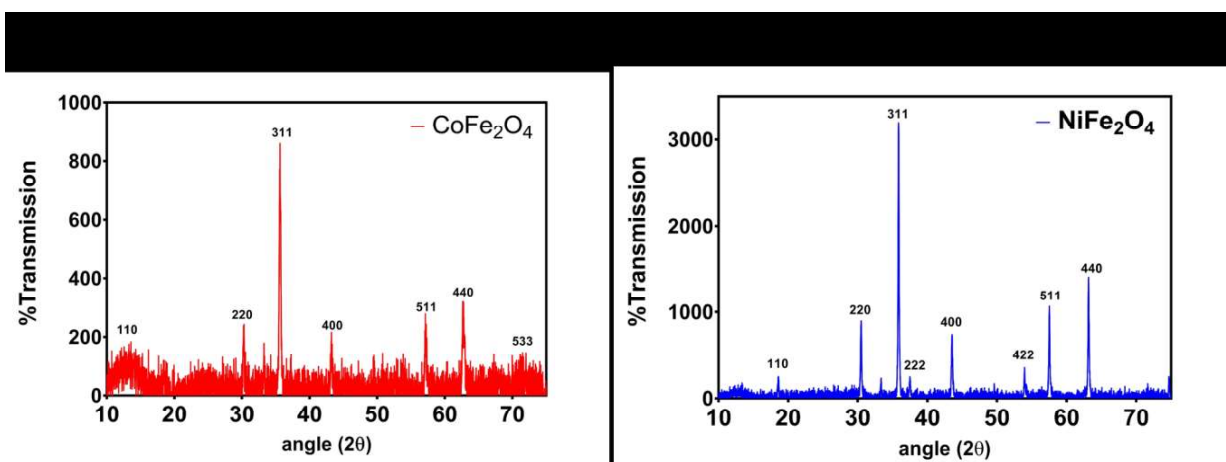


Figure 2. XRD images of (a) CoFe_2O_4 and (b) NiFe_2O_4 .

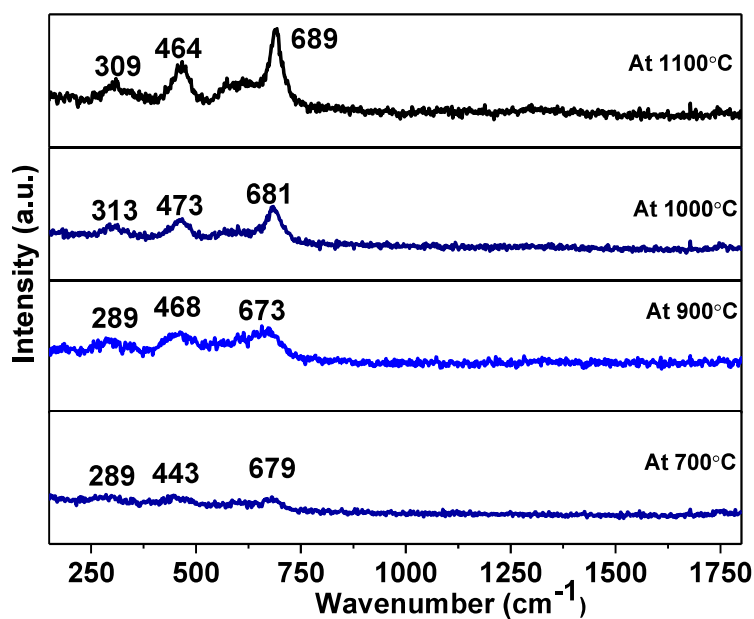


Figure 3. Raman Active Modes of CoFe_2O_4 nanoparticles as a function of temperature ($1100^\circ\text{C} - 700^\circ\text{C}$).

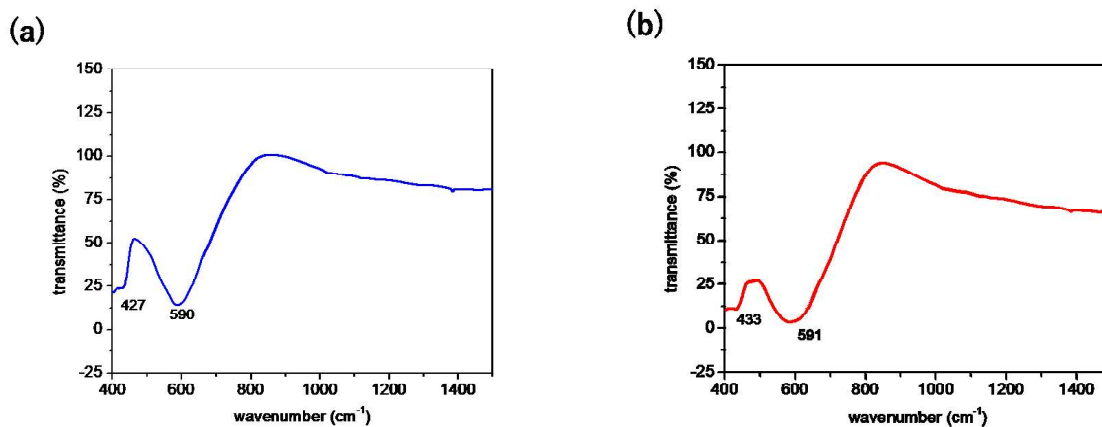
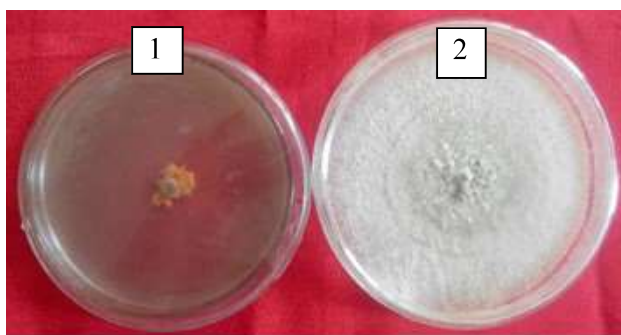
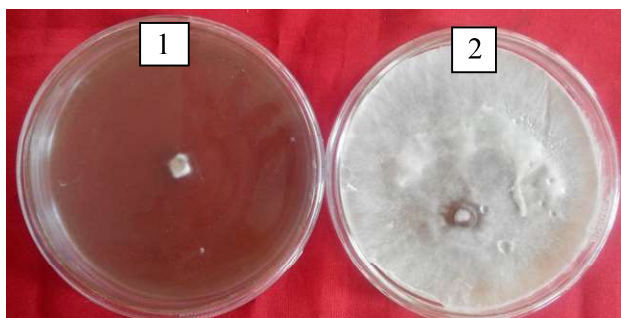


Figure 4. FTIR Transmission of (a) CoFe_2O_4 and (b) NiFe_2O_4 nanoparticles.

(a)



(b)



(c)

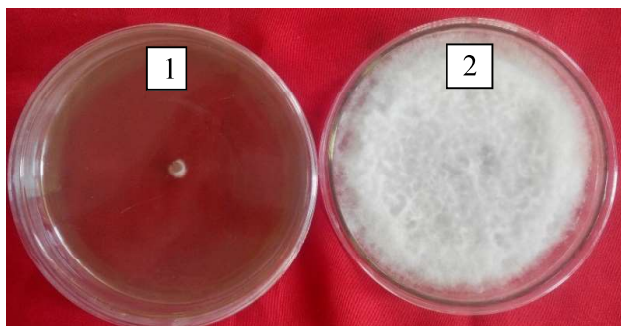


Figure 5. (a) Induction of microcycle conidiation in *Colletotrichum gloeosporioides* at (1) 500 ppm of nickel nanoparticles compared to (2) untreated control (b) Inhibitory effect of (1) nickel nanoparticles at 500 ppm compared to (2) untreated control on mycelia growth of *Dematophora necatrix*. (c) Inhibitory effect of nickel nanoparticles at 500 ppm (1) compared to untreated control (2) on mycelia growth of *Fusarium oxysporum*.



Figure 6. Effect of (a) CoFe_2O_4 and (b) NiFe_2O_4 ferrite nanoparticles against *Fusarium* wilt of capsicum under pot culture conditions compared to (c) control.

Table 1. *In vitro* efficacy of nanoparticles of (a) CoFe_2O_4 and (b) NiFe_2O_4 against mycelial growth of three different plant pathogenic fungi.

| <i>In vitro</i> efficacy of nanoparticles of CoFe_2O_4 | | | | | | | |
|--|--------------------------------|------------------|------------------|------------------|------------------|-------|--------------------|
| Plant pathogenic fungi | Mycelial growth inhibition (%) | | | | | | CD _{0.01} |
| | 100 ppm | 200 ppm | 300 ppm | 400 ppm | 500 ppm | Mean | |
| <i>Colletotrichum gloeosporioides</i> | 39.45 (38.89) | 46.39 (42.91) | 56.67 (48.82) | 77.23 (61.48) | 78.91 (62.63) | 59.73 | 1.03 |
| <i>Dematophora necatrix</i> | 39.44 (38.88) | 50.00 (44.98) | 59.45 (59.44) | 75.56 (60.35) | 88.90 (70.51) | 62.67 | 1.10 |
| <i>Fusarium oxysoprum</i> | 41.10 (39.77) | 50.28 (45.14) | 63.64 (52.92) | 75.84 (60.54) | 87.62 (69.37) | 63.70 | 4.29 |
| <i>In vitro</i> efficacy of nanoparticles of NiFe_2O_4 | | | | | | | |
| <i>Colletotrichum gloeosporioides</i> | 43.25 (41.10) | 54.06 (47.31) | 61.94 (51.89) | 78.06 (62.05) | 81.39 (64.42) | 63.74 | 1.04 |
| <i>Dematophora necatrix</i> | 43.61 (41.31) | 52.78 (46.57) | 61.39 (51.57) | 78.89 (62.64) | 93.33 (75.00) | 66.00 | 1.75 |
| <i>Fusarium oxysoprum</i> | 58.06 (49.63) | 60.28 (50.92) | 68.61 (55.92) | 83.33 (65.94) | 89.45 (71.02) | 71.95 | 2.35 |

*Note: Figures in parentheses are arcsine-transformed values

Table 2. Evaluation of CoFe_2O_4 and NiFe_2O_4 nanoparticles under pot culture conditions against *Fusarium* wilt of capsicum.

| Ferrite nanoparticles | Concentration (ppm) | Disease incidence (%) | Disease reduction (%) |
|----------------------------|---------------------|-----------------------|-----------------------|
| CoFe_2O_4 | 100 | 90.47 (75.18) | 9.54 |
| | 200 | 76.18 (61.54) | 23.83 |
| | 300 | 38.09 (37.39) | 61.92 |
| | 400 | 28.57 (32.57) | 71.43 |
| | 500 | 9.52 (10.77) | 90.49 |
| NiFe_2O_4 | 100 | 80.95 (68.95) | 19.07 |
| | 200 | 57.12 (49.07) | 42.88 |
| | 300 | 23.80 (28.94) | 76.21 |
| | 400 | 9.52 (10.77) | 90.49 |
| | 500 | 0.00 (0.00) | 100.00 |
| Control | -- | 100.00 (90.00) | -- |
| CD_(0.05) | | 20.56 | |

**Figures in the parentheses are arc sine transformed values*

Keywords: nanoferrite, nano-agriculture, nano-fertilizers, antifungal

ToC figure

